IEEE Photonics Journal
An IEEE Photonics Society Publication

Open Access

Greatly Enhanced Wall-Plug Efficiency of N-Polar AlGaN-Based Deep Ultraviolet Light-Emitting Diodes

Volume 13, Number 3, June 2021

Hongchang Tao
Shengrui Xu
Xiaomeng Fan
Jincheng Zhang
Yue Hao, *Senior Member, IEEE*

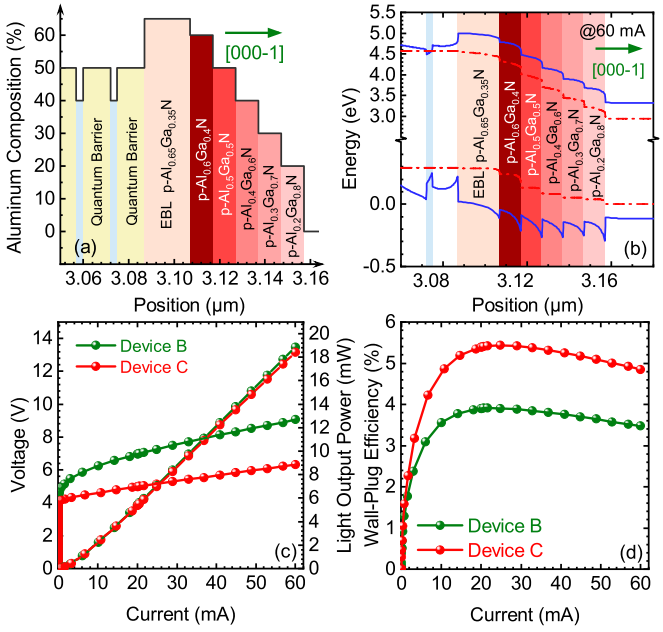

DOI: 10.1109/JPHOT.2021.3084752

IEEE photonics SOCIETY

IEEE

Greatly Enhanced Wall-Plug Efficiency of N-Polar AlGaN-Based Deep Ultraviolet Light-Emitting Diodes

Hongchang Tao, Shengrui Xu, Xiaomeng Fan, Jincheng Zhang, and Yue Hao, *Senior Member, IEEE*

State Key Discipline Laboratory of Wide Band Gap Semiconductor Technology, School of Microelectronics, Xidian University, Xi'an 710071, China

DOI:10.1109/JPHOT.2021.3084752

Manuscript received April 30, 2021; revised May 21, 2021; accepted May 25, 2021. Date of publication May 28, 2021; date of current version June 11, 2021. This work was supported in part by the National Key Research and Development Program of China under Grant 2016YFB0400801, in part by the National Natural Science Foundation of China under Grant 62074120, in part by the WuHu and Xidian University Special Fund for Industry-University-Research cooperation under Grant XWYCXY-012020007, in part by the State Key Laboratory on Integrated Optoelectronics under Grant IOSKL2018KF10, in part by the Fundamental Research Funds for the Central Universities under Grant JB211108, and in part by the Innovation Fund of Xidian University. Corresponding author: Shengrui Xu (e-mail: srxu@xidian.edu.cn).

Abstract: In this work, we numerically investigate the N-polar AlGaN-based deep ultraviolet light-emitting diodes (DUV LEDs) over the Ga-polar DUV LEDs. The light output power has increased from 7.1 mW of Ga-polar DUV LED to 18.8 mW of N-polar DUV LED at 60 mA, and the wall-plug efficiency (WPE) of N-polar DUV LED is boosted by 104% at 60 mA with the same structure of Ga-polar conventional DUV LED. Furthermore, the higher operation voltage of N-polar DUV LED induced by the large energy difference between the p-type interlayer and the p-GaN hole supplier is noted. To reduce the operation voltage of N-polar DUV LED, the structure with a staircase-like p-type interlayer is proposed. The incorporation of staircase-like aluminum composition p-type interlayer mitigates the large potential barrier for holes injection, and the operation voltage is comparable to the Ga-polar DUV LED. The reduced operation voltage further promotes the WPE of N-polar DUV LEDs. Thus, combined with the promoted electron blocking ability and the mitigated potential barrier for holes of N-polar DUV LED, the greatly enhanced WPE is as high as 4.9% at 60 mA, which is 2.88 times higher than the Ga-polar DUV LED.

Index Terms: Light-emitting diodes (LEDs), Deep-ultraviolet (DUV), N-polar.

1. Introduction

AlGaN-based deep ultraviolet light-emitting diodes (DUV LEDs) are deemed as the most promising candidate for environment-friendly DUV light sources [1]–[3]. In recent years, great interests have been generated for its application in UV medical curing, water disinfection, non-line-of-sight communication, and air sterilization [4]–[7]. At present, the predominant DUV light sources are based on mercury lamps. The portable size and low operation voltage make DUV LEDs widely integrated with common household appliances including air-condition and refrigerators. Nevertheless, DUV LEDs are currently suffering from low efficiency and unsatisfying optical power, though great progress has been made in the past few years [8]–[10]. Typically, DUV LED is more sensitive to the high-density threading dislocation, which can act as non-radiative recombination center and

leads to poor internal quantum efficiency (IQE) [11], [12]. Poor conductivity in p-type AlGaN due to high dopant ionization energy limits the hole injection efficiency into the active region and lead to more joule heat [13], [14]. Meanwhile, dominant transverse magnetic mode optical phonons and the adsorption of passive layers results in low light extraction efficiency (LEE) [15]. The external quantum efficiency co-affected by both the IQE and LEE thus deteriorates [16]. These technical challenges severely hinder the progress to fully replace the conventional mercury-based UV light sources. Furthermore, the quantum-confined stark effect and electron leakage are pronounced in AlGaN quantum wells [17],[18]. Insufficient hole concentration and feeble capability confining electrons significantly reduce the efficiency at high current injection levels. Therefore, electron leakage suppression and promoting hole injection efficiency are of great importance. Carrier transport of DUV LEDs is very sensitive to the energy band structure of the electron blocking layer (EBL) and multiple quantum wells (MQWs) [19], [20]. To promote carrier injection efficiency, various methods have been proposed through energy band engineering according to the review Ref. [20]. Combined with device structure modification and the utilization of polarization, the current injection efficiency has improved. As one of the most unique properties of III-nitrides, the lattice polarity is noteworthy in device performance. In contrast to metal-polar (Ga-polar) III-nitrides, N-polar III-nitride films have gained attention due to their distinct advantages including alleviated efficiency droop in the application of LEDs. The previous study revealed N-polar domains exhibit stronger photoluminescence intensity of AlGaN / GaN / AlGaN quantum well [21]. However, most researches focus on the DUV LEDs design based on Ga-polar, N-polar AlGaN-based DUV LEDs are rarely explored and not fully understood.

In this work, N-polar AlGaN-based DUV LEDs with a peak emission wavelength centered at ∼285 nm is investigated and compared with Ga-polar counterpart. The light output power, current-voltage (I-V) characteristics, and wall-plug efficiency (WPE) is obtained from simulation results. It is found that N-polar DUV LED greatly enhances the light output power and WPE. However, N-polar LED behaves higher operation voltage due to the larger potential barrier formed in the p-AlGaN interlayer. We also studied the output characteristics under the various aluminum composition of the p-AlGaN interlayer. A new staircase-like p-type AlGaN interlayer structure is proposed to mitigate the high operation voltage of N-polar DUV LEDs. In the staircase-like p-AlGaN interlayer, the Al composition is 60%, 50%, 40%, 30%, and 20% along [000-1] direction sequentially, each layer is 10 nm thick. The mitigated operation voltage confirms the new structure is favorable for WPE further promotion.

2. Device Structures and Simulation Parameters

To investigate the polarity-dependent characteristics of DUV LED. The experimental DUV LED fabricated by Yan et al is used as the reference structure in our work, which is grown along [0001] direction [22]. The DUV LED chip is square shaped of 400 μm × 400 μm. It is composed of a 3-μm-thick n-type $Al_{0.6}Ga_{0.4}N$ layer with the Si doping of 4×10^{18} cm^{-3} as the electron injection layer, and the activation energy is set to be 15 meV. Subsequently, five periods of $Al_{0.5}Ga_{0.5}N/Al_{0.4}Ga_{0.6}N$ MQWs are grown to emit DUV photons, of which the peak emission wavelength is 284.5 nm. The thickness for the $Al_{0.4}Ga_{0.6}N$ quantum wells and $Al_{0.5}Ga_{0.5}N$ quantum barriers is ∼3 nm and ∼12 nm, respectively. Then 20-nm-thick p-type $Al_{0.65}Ga_{0.35}N$ (Mg: 2×10^{19} cm^{-3}) is deposited to suppress electron leakage. Followed by a 50-nm-thick p-type $Al_{0.5}Ga_{0.5}N$ interlayer (Mg: 2×10^{19} cm^{-3}). Lastly, a heavily 120-nm-thick Mg-doped GaN (Mg: 1×10^{20} cm^{-3}) is grown as a contact layer. The hole injection layer is composed of three parts. The details of the DUV LED structure are schematically shown in Fig. 1.

To identify the in-depth origin for the carrier transport, the numerical calculation is performed with commercial software Advanced Physical Models of Semiconductor Devices (APSYS) based on finite element analysis. APSYS also adopts 6 × 6 k·p model for valence band calculation of strained wurtzite nitrides [23]. In the numerical simulation process, the ionization energy of p-dopant for GaN is 170 meV, while 470 meV for AlN [24], [25]. With the variation of Al content for $Al_xGa_{1-x}N$ alloy, the ionization energy linearly increases. The carrier transport is also sensitive

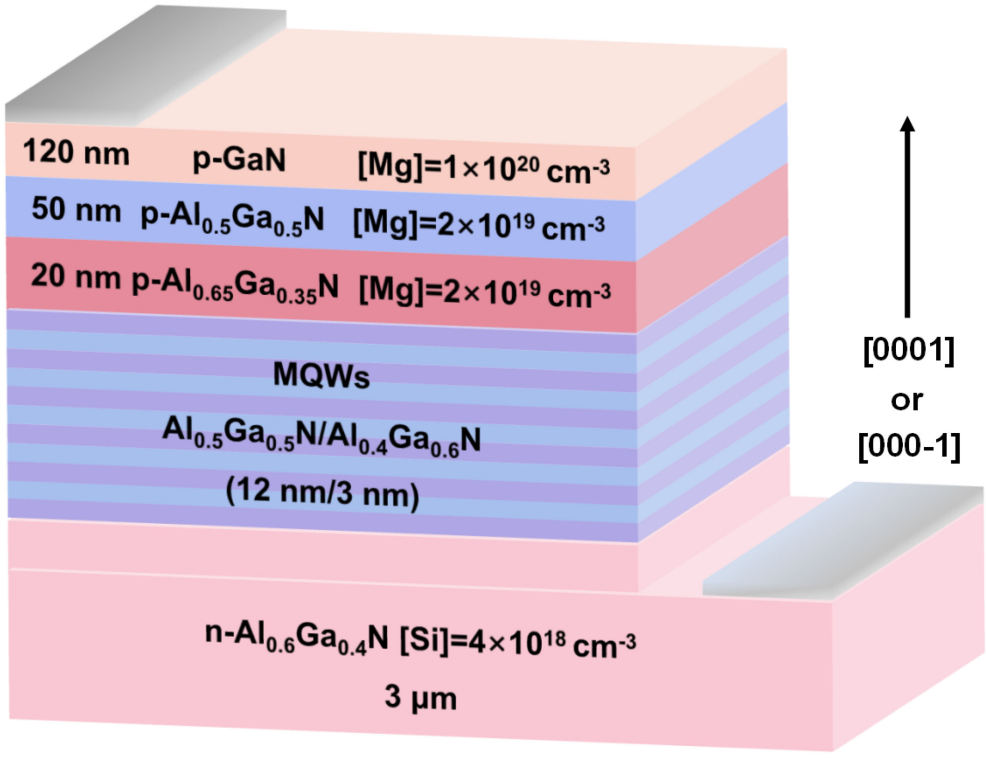

Fig. 1. Schematic diagram of the reference DUV LED structure, growth direction of Ga-polar is [0001] and of N-polar is [000-1].

to the energy band offset ratio, which is set to be 65/35 for AlGaN/AlGaN heterojunctions [26]. Based on methods developed by Fiorentini et al, polarization charges are calculated [27]. Since polarization charge can be screened by defect and dislocations, 50% of the theoretical polarization charges is considered in the device simulation [28]. Moreover, the Shockley-Read-Hall (SRH) recombination lifetime and Auger recombination coefficient are set to be 13 ns, 6.8×10^{-31} cm^6/s for nonradiative recombination in MQWs, respectively. The LEE of DUV LED is set to be 15%. The device simulation is calibrated with the measurement results of the fabricated device, and the parameters implemented is obtained through the curve-fitting procedure, which is a reasonable and feasible method [19]. The I-V characteristic is influenced by polarization charge screening coefficient, and the SRH lifetime as well as Auger recombination settings contribute to Light output power-Current (L-I) characteristics. The other material parameters of nitrides adopted in the simulation can be found elsewhere [29]. Also, tunneling process for holes and electrons are considered in our calculation by employing the transfer matrix method and the one-dimensional Schrödinger equation.

Firstly, the experimental and simulation results are shown in Fig. 2 [22]. It has shown that the calculated I-V and L-I curves are fitting well to the experimental data with parameters given above. Hence the physical model and simulation parameters is reliable. The calculated electroluminescence (EL) spectra shown in Fig. 2(c) reveal the peak emission wavelength is around ~284.5 nm at 20 mA and 60 mA, which is identical to the measurement results reported by Yan et al. Fig. 2(d) displays the calculated WPE with current increasing, which is determined by the I-V and L-I curves. It is noteworthy that the issue of efficiency droop is serious under large injection current. The WPE decreases from 2.89% of to 1.7% at 60 mA. However, such low efficiency cannot satisfy the demand of high power DUV applications. It is urgent to promote the WPE and alleviate the severe efficiency droop.

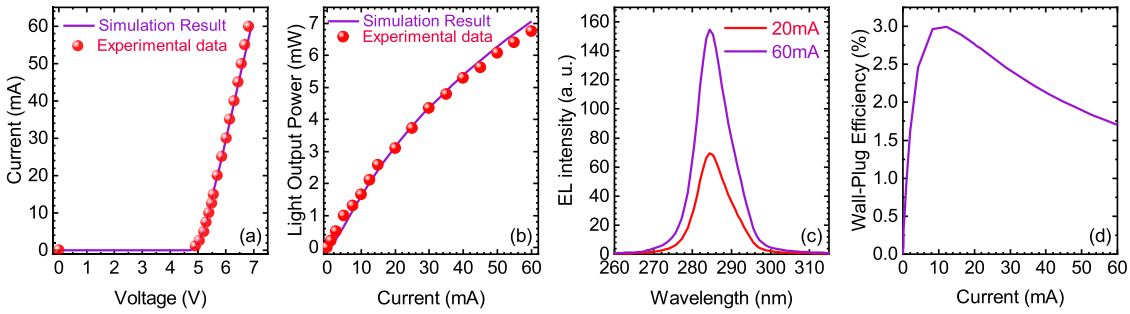

Fig. 2. Experimental and simulated (a) I-V, (b) L-I curve, and calculated (c) electroluminescence spectra and (d) wall-plug efficiency of the reference Ga-polar DUV LED (Device A).

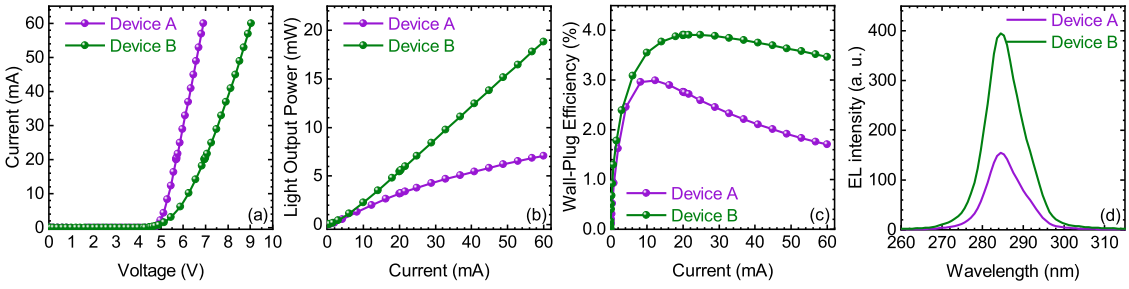

Fig. 3. (a) I-V, (b) L-I curve, (c) WPE, and (d) electro-luminescence spectra at 60 mA of Device A and B.

3. Results and Discussion

Based on the reference Ga-polar DUV LED structure (denoted as Device A), we investigate the N-polar DUV LED to probe the polarity effect, which is denoted as Device B here. Notably, the only difference between Device A and B is the lattice polarity, and the growth direction of Device A and B is along [0001] and [000-1], respectively.

As shown in Fig. 3, the I-V and L-I curves of Device A and B are presented. It is found that the devices turn on when the applied voltage is around 4 V and the turn-on current is approximately 1 μA. Once the device is on, Device B requires a higher voltage bias to reach the same current value compared with Device A in Fig. 3(a). In addition, the L-I curve of Device B exhibits a larger slope value, as well as the remarkable increase of light output power. Despite the marked enhancement of light output power, the WPE of Device B is also calculated to reveal the impact of higher operation voltage brought by the polarity inversion. Clearly, Device B features higher WPE in the whole current condition, and the two devices demonstrate efficiency droop under high injection current from Fig. 3(c). The droop value is defined as ($\mathrm{WPE_{max}}$-$\mathrm{WPE_{60\ mA}}$)/$\mathrm{WPE_{max}}$ $\times$ 100%, which reveals the degree of efficiency droop under high injection current. Remarkably suppressed efficiency droop is obtained of Device B, the droop value decreases from 43.1% of Device A to 11.2%, which indicates the superior electrons blocking capability of the N-polar structure. Notably, the type of polarization charge formed at heterointerfaces is opposite of Ga- and N-polar DUV LED. The polarization-induced electric-field strength differs only in direction for two devices. As a result, holes and electrons are accumulating in the opposite position of the quantum wells for two devices, and the photon energy could be innocent to the polarity condition. The calculated EL spectra identify the same peak emission wavelength of Device A and B under the injection current of 60 mA in Fig. 3(d). It is observed the EL intensity of Device B is boosted over 2 times compared

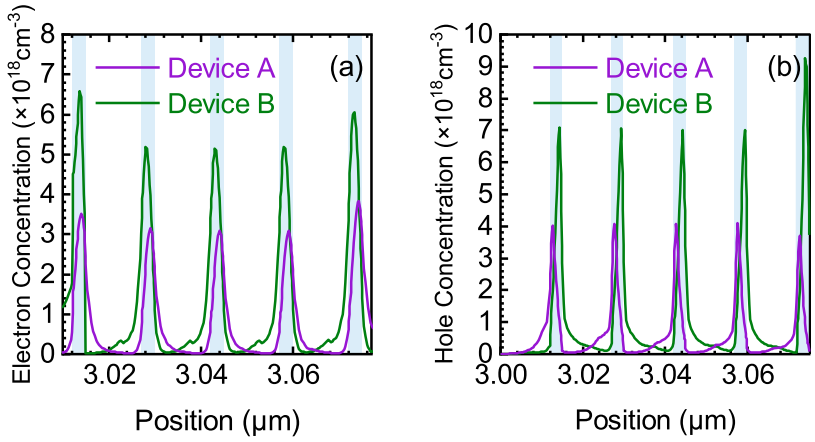

Fig. 4. (a) Electrons and (b) holes concentration distributions of Device A and B at 60 mA.

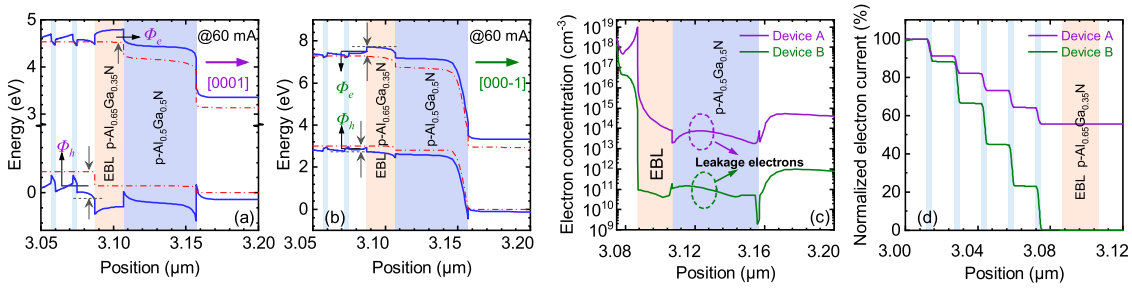

Fig. 5. Energy band diagrams of (a) Device A and (b) Device B. (c) Electron concentration profiles in the p-type regions, and (d) normalized electron current density for Device A and B. The data are all calculated at 60 mA.

with Device A. All the output performance shows the effectiveness for improved efficiency of N-polar DUV LED.

To explain the improved performance of Device B, Figs. 4(a) and (b) show the electrons and holes distribution profiles of the active region. The elevated hole and electron concentration of Device B indicate the enhanced carrier confinement ability and hole injection efficiency of the N-polar structure.

In order to illustrate the underlying mechanism regarding the improved performance, we plotted the energy band diagrams of two devices and explained them in detail. The energy band diagrams (blue lines) and quasi-Fermi levels (red dot dashed lines) of Device A and B under the injection current of 60 mA are illustrated in Figs. 5(a) and (b), respectively. For Device A, the positive polarization charge formed at the last quantum barrier (LQB)/EBL interface. Accordingly, the conduction band of LQB is significantly pulled down. The downward band leads to the significant electron overflowing and depletes holes. In addition, the titled valence band at LQB/EBL interface further increase the potential barrier height of holes besides the intrinsic barrier induced by the energy gap difference. In contrast to Device A, negative polarization charge is formed at the LQB/EBL of Device B, which elevates the conduction band and thus promotes the electron blocking ability. To reveal the capability of electrons blocking and the barrier for holes injection, we define the potential difference between conduction/valence band and the quasi- Fermi level as potential barrier height for electrons and holes, denoted by Φ_{e} and Φ_{h}, respectively. For Device A, the Φ_{e} is 288.89 meV and the Φ_{h} is 353.60 meV, while the promoted electron barrier for Device B is 456.98 meV, and the

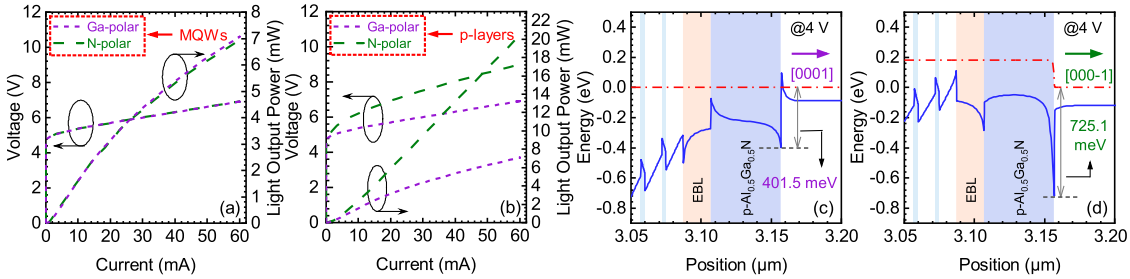

Fig. 6. I-V and L-I curves of the DUV LED structure that the (a) MQWs and (b) p-type region is N-polar or Ga-polar, respectively. Valence band diagrams of DUV LED for the p-type region is (c) Ga-polar and (d) N-polar at 4V. The other regions of the DUV-LED structure are all Ga-polar.

hole barrier height is mitigated to 268.82 meV. As a result, the significantly reduced potential barrier of holes enhances the hole injection to the active region. The accumulated negative polarization charges at the LQB/EBL deplete the electrons of Device B, and thus enhances the electron barrier compared to Device A, in which the positive charge is formed at the LQB/EBL interface. To reveal the electron leakage issue of DUV LED, which is detrimental for the efficiency droop, significantly reduced leakage electrons out of the active region are observed in Fig. 5(c). Fig. 5(d) presents the normalized electron current in the p-type layers, about 60% of electron current directly leaks into the p-type layers, whereas almost no leakage electron exists in Device B. Due to the enhanced output performance originated from elevated electron blocking capability and higher hole injection efficiency, Device B appears higher light output power and WPE.

In contrast to the Ga-polar structure of Device A, it is worth noting that Device B exhibits higher operation voltage shown in Fig. 3(a). Even though the light output power of N-polar device significantly improved, the promotion of WPE is not large as expected. The sacrifice of WPE promotion is ascribed to the higher operation voltage of the N-polar device. Therefore, further exploration is necessary to determine the physical mechanism of the increased voltage resulted from polarity inversion.

Since two regions are crucial for the carrier transport of DUV LEDs, one is the active region, i.e., multiple quantum barriers and wells, and the other is the p-type layers. The polarity inversion may have an impact on these regions according to the theoretical investigation [30], [31]. Based on the same structure shown in Fig. 1, we have simulated two structures to identify the dominant impact on the active region and p-type region, respectively. One structure is that the polarity of MQWs is modified to N-polar, leaving the polarity of other regions Ga-polar. While investigating the polarity influence of p-type regions, all the p-type regions change to N-polar, and the other regions stay Ga-polar. The calculated results of the modified MQWs polarity structure and p-type polarity structure are shown in Figs. 6(a) and (b), respectively. Notably, the operation voltage for MQWs with different polarity are almost the same. Also, the light output power of the structure with N-polar MQWs is the same as the Ga-polar structure. However, the significant difference in output performance is observed for the different polarity of p-type region. The output characteristic of the structure with N-polar p-type region is similar to Device B shown in Figs. 3(a) and (b). The calculation results shown in Fig. 6. indicate the increased operation voltage of the N-polar structure mainly drops on the p-type regions.

To clarify the origin of the large potential barrier at the p-type region for the N-polar structure. Consider the great voltage difference for N-polar and Ga-polar structures under the same current injection after the LEDs turn on, we have plotted the energy band diagrams of the p-type region of Ga polarity and N polarity at the same bias at 4 V in Figs. 6(c) and (d), respectively. The hole injection barrier of the Ga-polar p-type region is 401.5 meV while 725.1 meV for N-polar counterpart. Higher holes potential barrier originates from the positive polarization charge at the p-type interlayer/p-GaN interface of the N-polar structure, which depletes holes and hinders holes

injection. It is noted that tunneling process is considered within the delta-like energy barrier as shown in Figs. 6(c) and (d) in the whole current condition. Since holes at p-$Al_{0.5}Ga_{0.5}N$/p-GaN interface are accumulated at the p-GaN side of Ga-polar p-layer structure, the electric field formed within the p-$Al_{0.5}Ga_{0.5}N$ interlayer would increase the hole energy and thus promoted hole injection efficiency [32]. However, holes are depleted at the p-$Al_{0.5}Ga_{0.5}N$/p-GaN interface of N-polar p-type layers structure, the holes injection require higher bias voltage though tunneling process is included. As a result, increased voltage is necessary to overcome the large potential barrier of N-polar p-type structure, and the potential barrier also exists of Device B shown in Fig. 5(b), the results explain the larger bias voltage originates from the p-type interlayer of Device B reasonably.

From the calculated valence band diagrams in Fig. 6(d), the large potential barrier in the N-polar p-type region is formed at the p-interlayer/p-GaN interface. To mitigate the potential barrier, we investigate the output performance of the Ga-polar and N-polar DUV LED by varying the Al composition from 10% to 60%. As depicted in Fig. 7, the forward voltage, light output power, and WPE under the injection current 20 mA and 60 mA are presented. The trends for Ga- and N-polar structures are similar under different injection conditions. For Ga-polar DUV LED, the forward voltage drops first and then increases with Al composition increasing. The reason for this trend is that the p-type interlayer is the middle layer of the p-type region, once the Al composition is low, the potential barrier between EBL and p-type interlayer increases. Once the Al composition of the p-type interlayer is varied, the electric field induced by the hole depletion between EBL and p-type interlayer, as well as the hole depletion between p-type interlayer and p-GaN is altered. The holes are severely depleted for devices with Al composition of 10%, 20%, and 60%, which is due to the large energy difference between the interlayer and EBL as well as p-GaN, thus holes transportation is limited and results in the greater voltage of devices with Al composition of 10%, 20%, and 60%. While for the Al composition of 30%, 40%, and 50%, enough holes can be guaranteed, and the kinetic energy of holes increases attributed to the electric field in the depletion region [32]. The net work done to holes by the electric field enables holes to overcome the potential barrier. For devices with Al composition of 40%, the energy difference between the net work done by the electric field and the potential barrier is the greatest among these three devices, which indicates the larger kinetic of holes to transport. As a result, the forward voltage is the lowest for devices with Al composition of 40%. Since electron leakage is significant in Ga-polar DUV LED, the electron blocking capability promotes as the Al composition of p-type interlayer increases. The light output power and WPE increase monotonously. For N-polar DUV LED, the forward voltage varies with Al composition and the trend is like the Ga-polar counterpart, the lowest forward voltage is obtained for p-$Al_{0.4}Ga_{0.6}N$ interlayer. N-polar DUV LED exhibit stronger electron blocking capability as explained above. As a result, the light output power exhibits a slight difference varying with Al composition. The change of WPE is attributed to the modification of forward voltage for N-polar DUV LED. The maximum WPE at 60 mA is approximately 4% when the p-$Al_{0.4}Ga_{0.6}N$ interlayer is adopted for the N-polar structure.

However, the forward voltage of N-polar DUV-LED is relatively large. Since the forward voltage of N-polar DUV LED is significantly influenced by the p-type interlayer. The optimization of the p-type interlayer design is urgent to reduce the forward voltage for N-polar DUV LED. In order to mitigate the large energy difference between the p-type interlayer and p-GaN and avoid the large potential barrier between p-type interlayer and p-EBL caused by the aluminum composition reduction of the p-type interlayer. We design a staircase-like structure for the p-type interlayer, the original 50-nm-thick p-$Al_{0.5}Ga_{0.5}N$ layer of Device B changes to p-$Al_{0.6}Ga_{0.4}N$/$Al_{0.5}Ga_{0.5}N$/$Al_{0.4}Ga_{0.6}N$/$Al_{0.3}Ga_{0.7}N$/$Al_{0.2}Ga_{0.8}N$, the thickness of each layer is 10 nm. The schematic of aluminum composition at different position is shown in Fig. 8(a), and the corresponding energy diagram is also shown in Fig. 8(b). It is noted that the gradient reduction of aluminum composition along growth direction [000-1] is analogous to the staircase. The N-polar DUV LED structure with staircase-like p-type interlayer is denoted as Device C. As displayed in Fig. 8(c), the forward voltage is remarkably reduced with the introduction of a staircase-like p-type interlayer. The bias voltage under the injection current 60 mA is 6.33 V of Device C, which is smaller than the

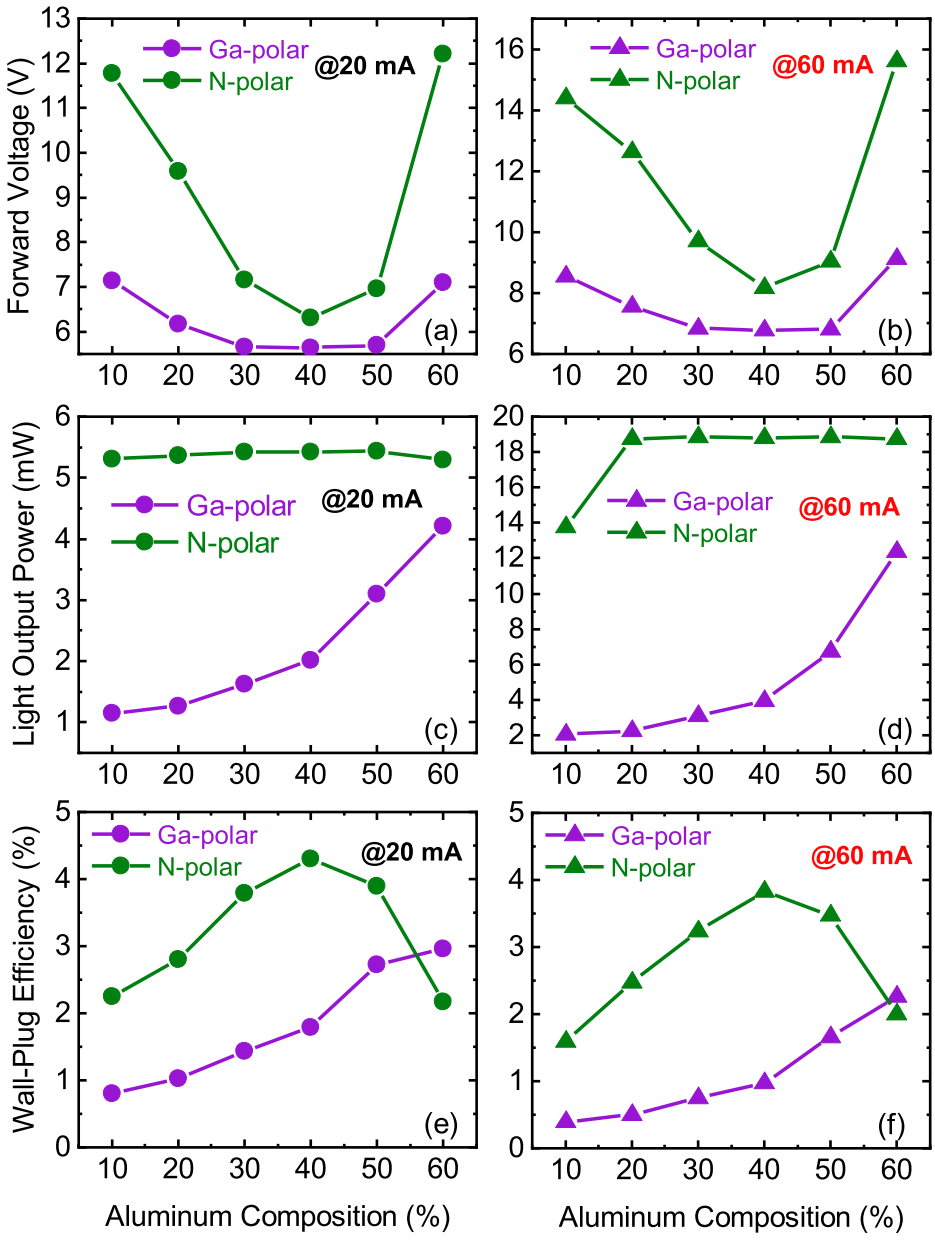

Fig. 7. The forward voltage, light output power, and wall-plug efficiency of Ga and N-polar DUV-LED composed of different aluminum composition of p-type interlayer at the injection current of (a) 20 mA and (b) 60 mA.

forward voltage 6.91 V of Device A under the same injection condition. Notably, the I-V slope of Device C is approaching Device A shown in Fig. 3(a), which indicates the significantly reduced potential barrier for holes Device C compared with Device B. For each p-$Al_xGa_{1-x}N$/p-$Al_yGa_{1-y}N$ ($x>y$) heterostructure along [000-1] direction, the holes depletion exists at the p-$Al_xGa_{1-x}N$ side, which is observed in Fig. 8(b). The depletion region of holes generates electric-field along [0001] direction in the p-$Al_xGa_{1-x}N$. Increased kinetic energy for holes is obtained due to the intrinsic electric field induced at the hetero-interfaces of the staircase-like p-type interlayer [32]. Therefore,

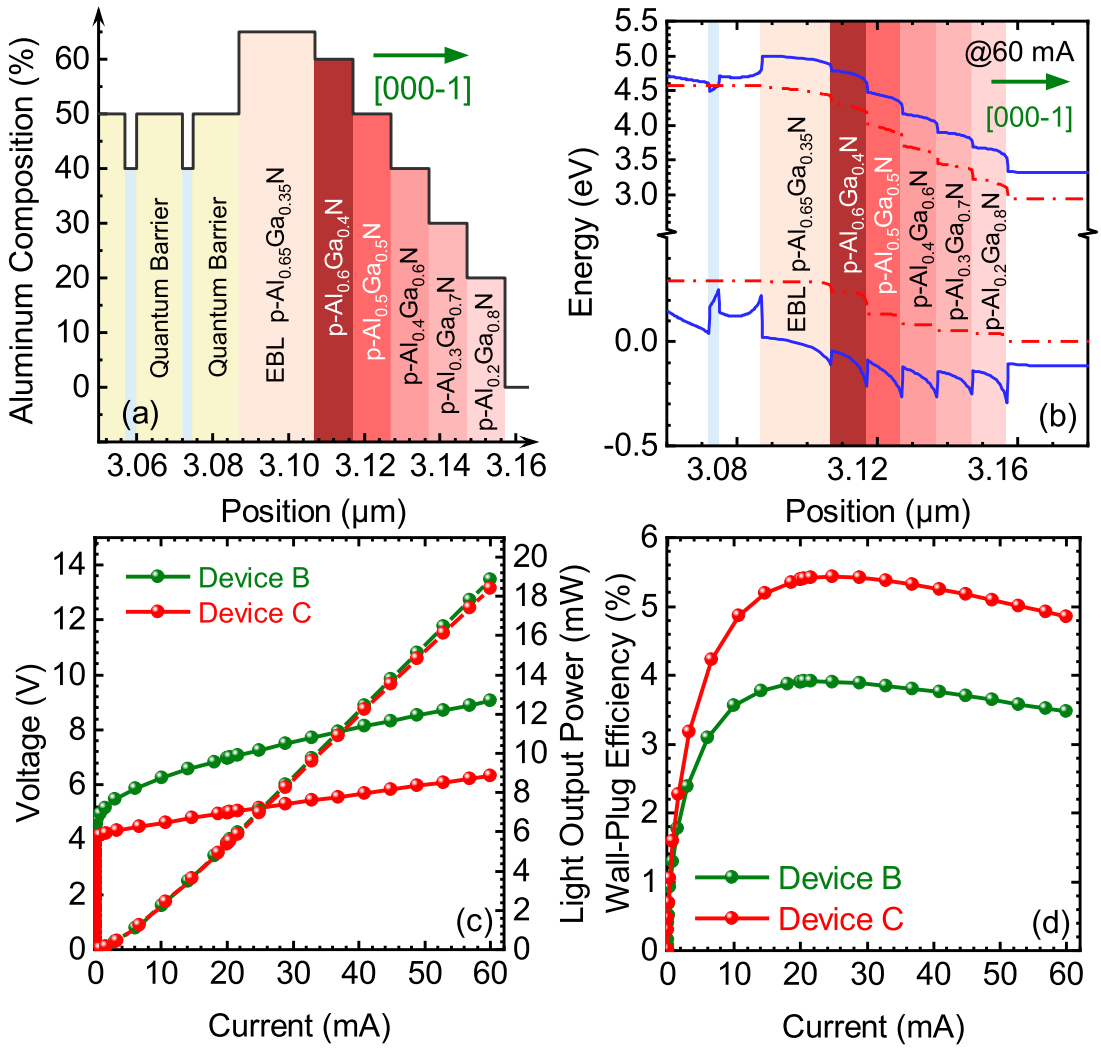

Fig. 8. (a) The schematic aluminum composition profiles of Device C along [000-1] direction. (b) Energy band diagrams of Device C at 60 mA. (c) I-V and L-I curves, and (d) WPE of Device B and C.

the enhanced kinetic energy of holes can overcome potential barrier formed at the p-$Al_xGa_{1-x}N$/p-$Al_yGa_{1-y}N$ (x>y) interfaces. Combined with the mitigated potential barrier at the p-$Al_{0.65}Ga_{0.35}N$ EBL/p-type interlayer and the p-type interlayer/p-GaN interfaces, the forward voltage of Device C thus reduces. As a result, through the reduction of power loss induced by the higher operation voltage, the WPE is significantly promoted indicated by Fig. 8(d). Combined with N-polar and the new staircase-like p-type interlayer structure, the WPE is increased from 1.7% of the Device A to 4.9% at 60 mA, which is 2.88 times promoted.

4. Conclusion

To summarize, this work has systematically investigated the N-polar DUV LED with a peak emission wavelength at ~285 nm. The simulation results of N-polar conventional DUV LED reveal its superior capability for blocking electrons due to the enhanced electron barrier of EBL. Thus, significantly reduced leakage electrons are observed compared with the Ga-polar DUV LED. The light output power of N-polar DUV LED has been significantly promoted by 2.8 times. Furthermore, we find that

higher operation voltage of N-polar DUV LED hinders the WPE improvement, which is attributed to the large potential barrier formed between the p-type interlayer and the p-GaN layer of the structure. So, a newly designed staircase-like p-type interlayer structure has been proposed to lower the operation voltage of N-polar DUV LED. Finally, the WPE at 60 mA increases from 1.7% to 4.9%, which is boosted by 188% compared with Ga-polar DUV LED. Our findings indicate that the N polarity has great potential for high-efficiency DUV LEDs. We believe the proposed DUV LED structure and the underlying device physics in this work are favorable for the advancement of DUV LEDs.

Acknowledgment

The authors wish to thank the anonymous reviewers for their valuable suggestions.

References

[1] M. Kneissl, T.-Y. Seong, J. Han, and H. Amano, "The emergence and prospects of deep-ultraviolet light-emitting diode technologies," *Nature Photon.*, vol. 13, no. 4, pp. 233–244, Mar. 2019.
[2] Y. Taniyasu, M. Kasu, and T. Makimoto, "An aluminium nitride light-emitting diode with a wavelength of 210 nanometres," *Nature*, vol. 441, no. 7091, pp. 325–328, May. 2006.
[3] H. Hirayama, N. Maeda, S. Fujikawa, S. Toyoda, and N. Kamata, "Recent progress and future prospects of algan-based high-efficiency deep-ultraviolet light-emitting diodes," *Jpn. J. Appl. Phys.*, vol. 53, no. 10, Oct. 2014, Art. no. 100209.
[4] K. Song, M. Mohseni, and F. Taghipour, "Application of ultraviolet light-emitting diodes (UV-LEDs) for water disinfection: A review," *Water Res.*, vol. 94, pp. 341–349, May. 2016.
[5] P. E. Hockberger, "A history of ultraviolet photobiology for humans, animals and microorganisms," *Photochem. Photobiol.*, vol. 76, no. 6, pp. 561–579, Dec. 2002.
[6] M. Kneissl and J. Rass, Eds., *III-Nitride Ultraviolet Emitters-Technology and Applications*. New York, NY, USA: Springer, 2015.
[7] Z. Xu and B. M. Sadler, "Ultraviolet communications: Potential and state-of-the-art," *IEEE Commun. Mag.*, vol. 46, no. 5, pp. 67–73, May. 2008.
[8] M. Shatalov *et al.*, "AlGaN deep-ultraviolet light-emitting diodes with external quantum efficiency above 10%," *Appl. Phys. Exp.*, vol. 5, no. 8, Aug. 2012, Art. no. 082101.
[9] T. Takano, T. Mino, J. Sakai, N. Noguchi, K. Tsubaki, and H. Hirayama, "Deep-ultraviolet light-emitting diodes with external quantum efficiency higher than 20% at 275 nm achieved by improving light-extraction efficiency," *Appl. Phys. Exp.*, vol. 10, no. 3, Mar. 2017, Art. no. 031002.
[10] N. Lobo-Ploch *et al.*, "Milliwatt power 233nm AlGaN-based deep UV-LEDs on sapphire substrates," *Appl. Phys. Lett.*, vol. 117, no. 11, Sep. 2020, Art. no. 111102.
[11] H. Hirayama *et al.*, "222-282 nm AlGaN and InAlGaN-based deep-UV LEDs fabricated on high-quality AlN on sapphire," *Phys. Status Solidi A-Appl. Mat.*, vol. 206, no. 6, pp. 1176–1182, Jun. 2009.
[12] M. Imura *et al.*, "Dislocations in AlN epilayers grown on sapphire substrate by high-temperature metal-organic vapor phase epitaxy," *Jpn. J. Appl. Phys.*, vol. 46, no. 4A, pp. 1458–1462, Apr. 2007.
[13] H. Tao, S. Xu, J. Zhang, P. Li, Z. Lin, and Y. Hao, "Numerical investigation on the enhanced performance of N-polar AlGaN-based ultraviolet light-emitting diodes with superlattice p-type doping," *IEEE Trans. Electron Devices.*, vol. 66, no. 1, pp. 478–484, Jan. 2019.
[14] M. Katsuragawa *et al.*, "Thermal ionization energy of Si and Mg in AlGaN," *J. Cryst. Growth.*, vol. 189, pp. 528–531, Jun. 1998.
[15] K. B. Nam, J. Li, M. L. Nakarmi, J. Y. Lin, and H. X. Jiang, "Unique optical properties of AlGaN alloys and related ultraviolet emitters," *Appl. Phys. Lett.*, vol. 84, no. 25, pp. 5264–5266, Jun. 2004.
[16] Y. Nagasawa and A. Hirano, "A review of AlGaN-based deep-ultraviolet light-emitting diodes on sapphire," *Appl. Sci.-Basel.*, vol. 8, no. 8, Aug. 2018, Art. no. 1264.
[17] Y. Kang *et al.*, "Efficiency droop suppression and light output power enhancement of deep ultraviolet light-emitting diode by incorporating inverted-v-shaped quantum barriers," *IEEE Trans. Electron Devices.*, vol. 67, no. 11, pp. 4958–4962, Nov. 2020.
[18] Z.-H. Zhang *et al.*, "Increasing the hole energy by grading the alloy composition of the p-type electron blocking layer for very high-performance deep ultraviolet light-emitting diodes," *Photon. Res.*, vol. 7, no. 4, pp. B1–B6, Apr. 2019.
[19] Y. Kuo, F. Chen, J. Chang, M. Huang, B. Liou, and Y. Shih, "Design and optimization of electron-blocking layer in deep ultraviolet light-emitting diodes," *IEEE J. Quantum Electron.*, vol. 56, no. 1, Feb. 2020, Art. no. 3300206.
[20] Z. J. Ren *et al.*, "Band engineering of III-nitride-based deep-ultraviolet light-emitting diodes: A review," *J. Phys. D-Appl. Phys.*, vol. 53, no. 7, Feb. 2020, Art. no. 073002.
[21] W. Guo *et al.*, "Lateral-polarity structure of AlGaN quantum wells: A promising approach to enhancing the ultraviolet luminescence," *Adv. Funct. Mater.*, vol. 28, no. 32, Aug. 2018, Art. no. 1802395.
[22] J. Yan *et al.*, "AlGaN-based deep-ultraviolet light-emitting diodes grown on high-quality AlN template using MOVPE," *J. Cryst. Growth.*, vol. 414, pp. 254–257, Mar. 2015.
[23] S. L. Chuang, and C. S. Chang, "k·p method for strained wurtzite semiconductors," *Phys. Rev. B, Condens. Matter.*, vol. 54, no. 4, pp. 2491–2504, Jul. 1996.

[24] W. Götz, N. M. Johnson, J. Walker, D. P. Bour, and R. A. Street, "Activation of acceptors in Mg-doped GaN grown by metalorganic chemical vapor deposition," *Appl. Phys. Lett.*, vol. 68, no. 5, pp. 667–669, Aug. 1998.
[25] J. Piprek, "Origin of InGaN/GaN light-emitting diode efficiency improvements using tunnel-junction-cascaded active regions," *Appl. Phys. Lett.*, vol. 104, no. 5, Feb. 2014, Art. no. 051118.
[26] D. R. Hang, C. H. Chen, Y. F. Chen, H. X. Jiang, and J. Y. Lin, "$Al_xGa_{1-x}N$/GaN band offsets determined by deep-level emission," *J. Appl. Phys.*, vol. 90, no. 4, pp. 1887–1890, Aug. 2001.
[27] V. Fiorentini, F. Bernardini, and O. Ambacher, "Evidence for nonlinear macroscopic polarization in III-V nitride alloy heterostructures," *Appl. Phys. Lett.*, vol. 80, no. 7, pp. 1204–1206, Feb. 2002.
[28] F. Renner, P. Kiesel, G. H. Döhler, M. Kneissl, C. G. Van de Walle, and N. M. Johnson, "Quantitative analysis of the polarization fields and absorption changes in InGaN/GaN quantum wells with electro absorption spectroscopy," *Appl. Phys. Lett.*, vol. 81, no. 3, pp. 490–492, Jul. 2002.
[29] I. Vurgaftman and J. R. Meyer, "Band parameters for nitrogen-containing semiconductors," *J. Appl. Phys.*, vol. 94, no. 6, pp. 3675–3696, Sep. 2003.
[30] Y.-K. Kuo, J.-Y. Chang, H.-T. Chang, F.-M. Chen, Y.-H. Shih, and B.-T. Liou, "Polarization effect in algan-based deep-ultraviolet light-emitting diodes," *IEEE J. Quantum Electron.*, vol. 53, no. 1, Dec. 2016, Art. no. 3300106.
[31] H. Jia *et al.*, "Investigation of quantum structure in N-polar deep-ultraviolet light-emitting diodes," *J. Appl. Phys.*, vol. 129, no. 13, Art. no. 133102, Apr. 2021.
[32] Z.-H. Zhang *et al.*, "On the electric-field reservoir for III-nitride based deep ultraviolet light-emitting diodes," *Opt. Exp.*, vol. 25, no. 14, pp. 16550–16559, Jul. 2017.